

# Selection and gene flow shape genomic islands that control floral guides

Hugo Tavares<sup>a,1</sup>, Annabel Whibley<sup>a</sup>, David L. Field<sup>b,c</sup>, Desmond Bradley<sup>a</sup>, Matthew Couchman<sup>a</sup>, Lucy Copsy<sup>a</sup>, Joane Elleouet<sup>a</sup>, Monique Burrus<sup>d</sup>, Christophe Andalo<sup>d</sup>, Miaomiao Li<sup>e,f,g</sup>, Qun Li<sup>e,f</sup>, Yongbiao Xue<sup>e,f,g,h</sup>, Alexandra B. Rebocho<sup>a</sup>, Nicolas H. Barton<sup>b,2</sup>, and Enrico Coen<sup>a,2</sup>

<sup>a</sup>Department of Cell and Developmental Biology, John Innes Centre, NR4 7UH Norwich NR4 7UH, United Kingdom; <sup>b</sup>Institute of Science and Technology Austria, 3400 Klosterneuburg, Austria; <sup>c</sup>Department of Botany and Biodiversity Research, Faculty of Life Sciences, University of Vienna, A-1030 Vienna, Austria; <sup>d</sup>Laboratoire Evolution et Diversité Biologique, UMR 5174 CNRS–Université Paul Sabatier, 31062 Toulouse Cédex 9, France; <sup>e</sup>State Key Laboratory of Molecular Developmental Biology, Institute of Genetics and Developmental Biology, Chinese Academy of Sciences, 100101 Beijing, China; <sup>f</sup>National Center for Plant Gene Research, Chinese Academy of Sciences, 100101 Beijing, China <sup>g</sup>School of Life Sciences, University of Chinese Academy of Sciences, 100190 Beijing, China; and <sup>h</sup>Beijing Institute of Genomics, Chinese Academy of Sciences, 100101 Beijing, China

Edited by Nils Chr. Stenseth, University of Oslo, Oslo, Norway, and approved September 12, 2018 (received for review February 6, 2018)

**Genomes of closely-related species or populations often display localized regions of enhanced relative sequence divergence, termed genomic islands. It has been proposed that these islands arise through selective sweeps and/or barriers to gene flow. Here, we genetically dissect a genomic island that controls flower color pattern differences between two subspecies of *Antirrhinum majus*, *A.m.striatum* and *A.m.pseudomajus*, and relate it to clinal variation across a natural hybrid zone. We show that selective sweeps likely raised relative divergence at two tightly-linked *MYB*-like transcription factors, leading to distinct flower patterns in the two subspecies. The two patterns provide alternate floral guides and create a strong barrier to gene flow where populations come into contact. This barrier affects the selected flower color genes and tightly-linked loci, but does not extend outside of this domain, allowing gene flow to lower relative divergence for the rest of the chromosome. Thus, both selective sweeps and barriers to gene flow play a role in shaping genomic islands: sweeps cause elevation in relative divergence, while heterogeneous gene flow flattens the surrounding “sea,” making the island of divergence stand out. By showing how selective sweeps establish alternative adaptive phenotypes that lead to barriers to gene flow, our study sheds light on possible mechanisms leading to reproductive isolation and speciation.**

hybrid zone | *Antirrhinum* | genomic island | selective sweep | speciation

Genome scans of closely-related species or populations have revealed “genomic islands” as peaks of high relative sequence divergence ( $F_{st}$ ) that stand out against a lower “sea” of divergence (1–5). The causes of genomic islands remain unclear, but they have been suggested to contain key loci involved in local adaptation and/or reproductive isolation (6). However, their significance for speciation with or without gene flow between populations is a matter of debate (6–9). One hypothesis is that gene flow is unimpeded across most of the genome, reducing between-population diversity, except for loci under divergent selection and loci in close physical linkage to selected loci (8). Another hypothesis is that genomic islands reflect selective sweeps, where specific alleles are driven to high frequency, thus reducing within-population diversity (7, 9, 10). These two hypotheses are typically presented as alternatives, although they are not mutually exclusive: both barriers to gene flow and selective sweeps may play a role. Here, we determine how these processes contribute to a genomic island that controls floral differences between two subspecies of *Antirrhinum majus*: *A.m.striatum* and *A.m.pseudomajus*. This system has the advantage of being genetically tractable and having a hybrid zone that allows selection and gene flow to be analyzed in nature (11, 12).

*Antirrhinum* has closed flowers that are prised open by pollinating bees. *A.m.striatum* and *A.m.pseudomajus* exhibit two different floral patterns that signpost the bee entry point (Fig. 1 A and B). *A.m.striatum* flowers have restricted veins of magenta anthocyanin on upper petals, which contrast against a yellow

aurene background (Fig. 1A). *A.m.pseudomajus* exhibits a complementary pattern, with a patch of yellow at the bee entry point on lower petals contrasted against magenta (Fig. 1B). Yellow patterning is controlled by *SULF* (12). Here we focus on control of magenta by the *ROSEA* (*ROS*) and *ELUTA* (*EL*) loci (13–15). The advantage of studying these loci is that they are tightly linked, allowing variation in intervening regions to provide insights into evolutionary forces. A further locus influencing magenta pigmentation pattern is *VENOSA*, which promotes magenta in dorsal veins (14). Many natural accessions carry *VEN* alleles, while the cultivated species *A. majus* used for genetic analysis typically carries *ven*, allowing its effects to be seen in genetic crosses.

Flowers homozygous for recessive alleles at all three loci (*ros* *el* *ven*) have very weak magenta pigmentation (Fig. 1C). Introduction of *VEN* leads to magenta overlying the veins of dorsal petals (Fig. 1D), whereas introduction of *ROS* leads to strong magenta throughout the corolla (Fig. 1E). The semidominant *EL* allele restricts the magenta conferred by *VEN* and *ROS* to lie over the bee entry point (Fig. 1 F and G). The *ROS* locus contains three *MYB*-like transcription factors, *ROS1*, *ROS2*, and *ROS3*, with ~90% protein sequence identity in the MYB domain. So far, only *ROS1* and *ROS2* have been functionally characterized, with *ROS1* exerting the major control on anthocyanin levels and pattern (14).

## Significance

**Populations often show “islands of divergence” in the genome. Analysis of divergence between subspecies of *Antirrhinum* that differ in flower color patterns shows that sharp peaks in relative divergence occur at two causal loci. The island is shaped by a combination of gene flow and multiple selective sweeps, showing how divergence and barriers between populations can arise and be maintained.**

Author contributions: H.T., A.W., D.L.F., N.H.B., and E.C. designed research; H.T., A.W., D.L.F., D.B., M.C., L.C., J.E., and A.B.R. performed research; H.T., A.W., D.L.F., D.B., M.C., L.C., M.B., C.A., M.L., Q.L., Y.X., and N.H.B. contributed new reagents/analytic tools; H.T., A.W., D.L.F., M.C., M.L., N.H.B., and E.C. analyzed data; and H.T., A.W., N.H.B., and E.C. wrote the paper.

The authors declare no conflict of interest.

This article is a PNAS Direct Submission.

This open access article is distributed under [Creative Commons Attribution-NonCommercial-NoDerivatives License 4.0 \(CC BY-NC-ND\)](https://creativecommons.org/licenses/by-nc-nd/4.0/).

Data deposition: The genomic sequence data reported in this paper are available at European Nucleotide Archive (ENA), <https://www.ebi.ac.uk/ena> (accession no. ENA PRJEB28287), and the RNAseq data have been deposited in the Gene Expression Omnibus (GEO) database, <https://www.ncbi.nlm.nih.gov/geo> (accession no. GSE118621).

<sup>1</sup>Present address: Sainsbury Laboratory, University of Cambridge, Cambridge, United Kingdom.

<sup>2</sup>To whom correspondence may be addressed. Email: Nick.Barton@ist.ac.at or enrico.coen@jic.ac.uk.

This article contains supporting information online at [www.pnas.org/lookup/suppl/doi:10.1073/pnas.1801832115/-DCSupplemental](http://www.pnas.org/lookup/suppl/doi:10.1073/pnas.1801832115/-DCSupplemental).

Published online October 8, 2018.





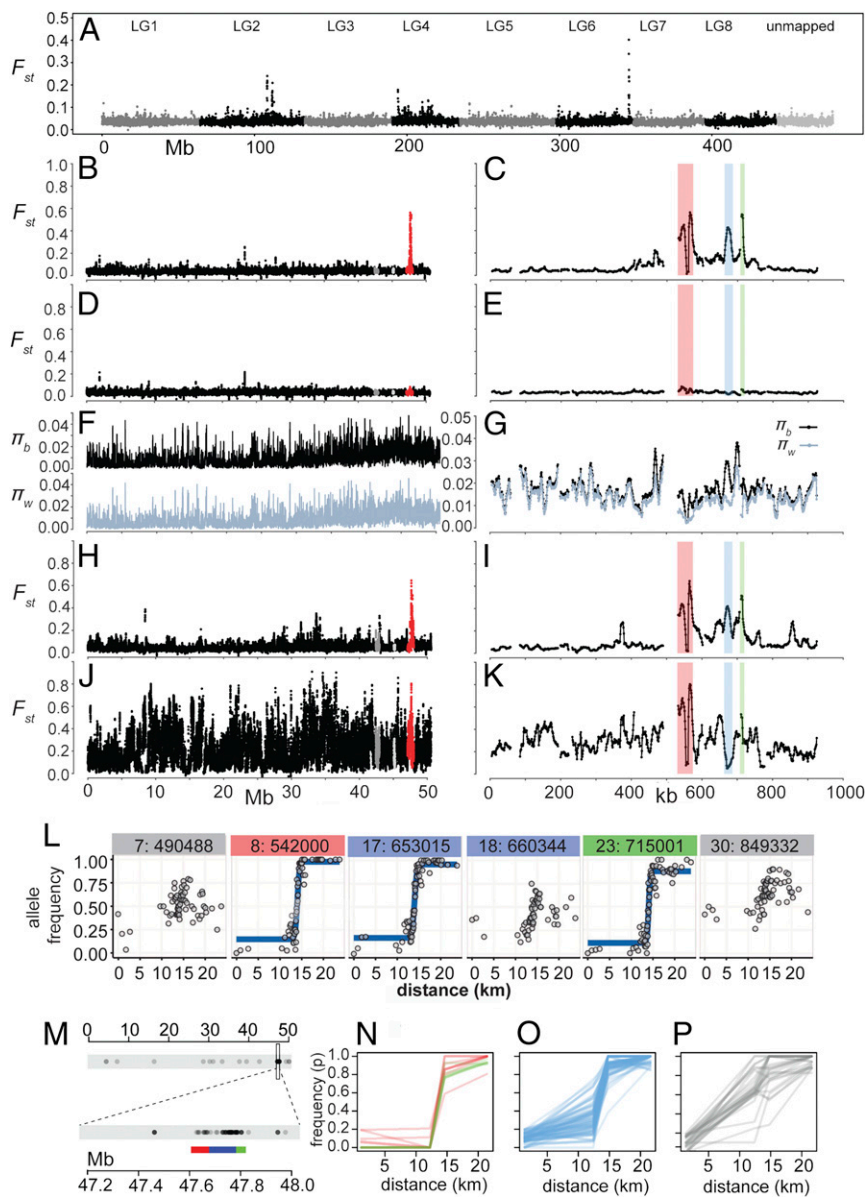


**Fig. 2.** Divergence between *A.m.striatum* and *A.m.pseudomajus*. (A)  $F_{st}$  comparisons between pools of *A.m.striatum* and *A.m.pseudomajus* populations either side of a hybrid zone (YP1 vs. MP2) and  $\sim 2.5$  km apart across the whole genome summarized in 50-kb windows with a 25-kb step size. (B) Same pools as A at 10-kb window resolution with 1-kb step size for chromosome 6. A region of high  $F_{st}$  is within a  $\sim 930$ -kb scaffold containing the *ROS* gene (red). Linked scaffolds contain *DICHOTOMA* (dark gray) and *PALLIDA* (light gray). (C) Closeup of region of high  $F_{st}$  at *ROS* comprising three peaks: left (red, 530–575 kb), middle (blue, 663–687 kb), and right (green, 707–720 kb on the *ROS* scaffold). The  $\sim 930$ -kb scaffold corresponds to positions 47.088–48.015 Mb on chromosome 6. (D and E) Pools from the same side of the hybrid zone (YP1 vs. YP2, both *A.m.striatum*, 0.2 km apart). (F and G)  $\pi_b$  and mean  $\pi_w$  for the same sequence data as used in B and C. (H and I) Pools sampled from populations either side of the hybrid zone (YP4 vs. MP11),  $\sim 20$  km apart. (J and K) Pools sampled from remote populations ( $\sim 100$  km apart, ML vs. CIN). (L) Clines for selected SNPs genotyped across the hybrid zone population. Headings denote the SNP identifier and position within the *ROS* 930-kb scaffold. (M) Distribution of 115 differential SNPs showing allele frequency differences  $>0.8$  between the outer pools (YP4 and MP11) and coverage of 20–200 $\times$  in all pools. Enlarged Inset shows regions corresponding to *ROS* peak (red), intervening region (blue), and *EL* peak (green). (N) SNP allele frequencies in the pools for eight differential SNPs within the *ROS* peak (red) and six within the *EL* peak (green) exhibit clines centered at the hybrid zone. (O) Most of the 74 SNPs located within the interval between the *ROS* and *EL* peaks, plotted in blue, exhibit clines centered at the hybrid zone. (P) SNP frequencies outside the *ROS* and *EL* peaks derive from flanking regions on the *ROS* superscaffold ( $n = 13$ ) or elsewhere on LG6 ( $n = 14$ ).

same order as the genome-wide average of 1.8 cM/Mbp. No phenotypic effect mapped to the middle  $F_{st}$  peak.

To determine whether the flower color phenotypes reflect variation in gene expression levels, we performed RNAseq on flower buds from homozygous progeny of individuals used in the genetic mapping experiments. Two of fifteen genes detected in the *ROS-EL* region showed highly significant expression differences (Fig. 4I,  $q < 0.001$ ; SI Appendix, Fig. S6). One transcript derived from *ROS1* and was about 10 times more abundant for samples with a dominant *ROS* allele compared with those with recessive *ros*, consistent with *ROS* conferring strong magenta. The second differential transcript encoded a *MYB*-like transcription factor with 57% protein identity to *ROS1* in the MYB domain and mapped to the *EL* region (SI Appendix, Figs. S5 and S6). This *EL-MYB* was expressed about threefold more in samples with a dominant *EL* allele compared with those with recessive *el*, consistent with it being a repressor of magenta pigmentation (SI Appendix, Fig. S6C). These results indicate that *EL* encodes a *MYB*-like transcription factor and show that at least some of the differences in gene activity are transcriptional. The *EL-MYB* gene maps to the rightmost  $F_{st}$  peak (Fig. 4A). Two other transcripts showed differences in expression between *el*

and *EL* genotypes (genes 5 and 14, Fig. 4I,  $q < 0.01$ ,  $q < 0.05$ , respectively) but showed a much weaker correlation with genotype than the *EL-MYB* gene (SI Appendix, Fig. S6 B and C).

We also analyzed recombinants, termed *ROS1\**, with breakpoints just downstream of the *ROS1* gene (Fig. 4H). *ROS1\** is expressed at a similar level to *A.m.pseudomajus ROS1*, although it carries the *ROS1* coding and upstream region of *A.m.striatum* (SI Appendix, Fig. S6C). Thus, variation in *ROS1* transcript levels largely maps to a downstream enhancer. The paler flowers of *ROS1\** compared with *A.m.pseudomajus ROS1* (Fig. 1E vs. Fig. 1H) suggests that variation in the coding region also contributes to the phenotype. Taken together with the observation of low  $\pi_w$  for only the left and right  $F_{st}$  peaks, these findings suggest that selective sweeps at *ROS* and *EL* caused these  $F_{st}$  peaks.

**Gene Flow Lowers  $F_{st}$  Outside the *ROS/EL* Region.** Sequence pools for populations of *A.m.pseudomajus* and *A.m.striatum* away from the center of the hybrid zone ( $\sim 20$  km apart instead of  $\sim 2.5$  km) showed a higher median  $F_{st}$  ( $0.048 \pm 0.0008$  compared with  $0.040 \pm 0.0004$ ) and more variable profile for chromosome 6 than for nearby populations (Figs. 2H and I, 3B, and 5). By contrast,  $F_{st}$  values at *ROS*, *EL*, and the intervening region were similar to

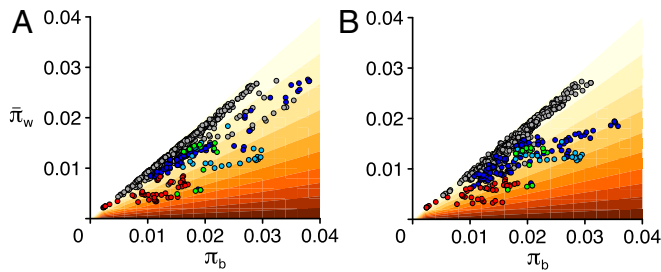


**Fig. 3.** Comparison of within- and between-population divergence in the *ROS/EL* region. Relationship between  $\pi_b$  and  $\pi_w$  for pools sampled either side of the hybrid zone, separated by  $\sim 2.5$  km (A, YP1 and MP2, corresponding to Fig. 2 B and C) or  $\sim 20$  km (B, YP4 and MP11, corresponding to Fig. 2 H and I), summarized in 10-kb windows, with a color gradient indicating the respective  $F_{st}$  (light colors, low; dark colors, high). The left, middle, and right  $F_{st}$  peaks indicated in Fig. 2C are shown as red, light blue, and green points, respectively. The dark blue points indicate windows between those  $F_{st}$  peaks. Other windows from around the *ROS* region are shown in gray.

those for the nearby populations (Figs. 2 H and I and 5). More remote populations showed a further increase in  $F_{st}$  for chromosome 6, with some comparisons yielding numerous  $F_{st}$  peaks, so that those at *ROS* and *EL* no longer stood out (Figs. 2 J and K and 5 and *SI Appendix*, Fig. S3 A and D and Table S9). Such a pattern of “isolation by distance” is often seen and indicates that gene flow reduces local divergence. In contrast,  $F_{st}$  is elevated across the whole *ROS/EL* region (Fig. 5), as expected from a strong barrier to gene flow generated by selection on *ROS* and *EL* (28). The statistical significance of these patterns is considered in *SI Appendix*, Supplementary Text S1.3.

A barrier to gene flow is also expected to cause sharp clines at any loci within it, regardless of whether they are selected. Indeed, we observe sharp clines at all divergent SNPs within or near the genomic islands, including those that lie outside *ROS* or *EL* (Fig. 2 L and *SI Appendix*, Supplementary Text S2 and Fig. S7). Of the  $\sim 6 \times 10^5$  biallelic SNPs on chromosome 6, 115 showed frequency differences greater than 0.8 between the outer pools ( $\sim 20$  km apart). One hundred and one of these differential SNPs were within an  $\sim 0.5$  Mbp *ROS/EL* region (Fig. 2 M and *SI Appendix*, Fig. S3 C), 14 of which were within the *ROS* and *EL*  $F_{st}$  peaks, 74 were between these peaks, and 13 were in flanking regions. Comparing SNP allele frequencies in the pools showed that the 14 differential SNPs within the *ROS* and *EL*  $F_{st}$  peaks, together with most of the 74 SNPs from the intervening region, exhibited clines centered at the hybrid zone (Fig. 2 N and O), confirmed and further refined by individual genotyping (Fig. 2 L and *SI Appendix*, Fig. S7). The remaining differential SNPs, including 14 that were distributed sparsely along the chromosome (Fig. 2 M), mainly showed a frequency change over a geographic region where the population density is low (Fig. 2 P and *SI Appendix*, Fig. S7 C). The change in frequency for these SNPs likely reflects fluctuations caused by the reduced gene flow created by the population density gap.

These findings support the hypothesis of a selective barrier at the *ROS/EL* region. The yellow flower patterning gene *SULF* exhibits steep SNP clines centered at the same geographical location as *ROS-EL* clines (12), supporting the idea that selection on flower color is the basis of the barrier.

Based on the 0.5-cM distance between *ROS* and *EL*, recombinants should be generated at hybrid zones, at a rate of 0.5% per heterozygote. Genotyping 2,393 individuals at the hybrid zone, using haplotype-specific markers in *ROS1* and *EL*, identified 201 recombinant haplotypes, which reached  $\sim 10\%$  frequency at the center of the hybrid zone (Fig. 4 J and K). Genotyping and test-crossing of progeny grown from 27 recombinants confirmed that most gave the expected phenotypes (*SI Appendix*, Supplementary Text S3). Assuming a neutral model with no selection against recombinants, we estimated a lower bound of  $\sim 85$  generations for the age of this hybrid zone (*SI Appendix*, Supplementary Text S4). If the hybrid zone is older than this, then selection must have acted to eliminate recombinants. A

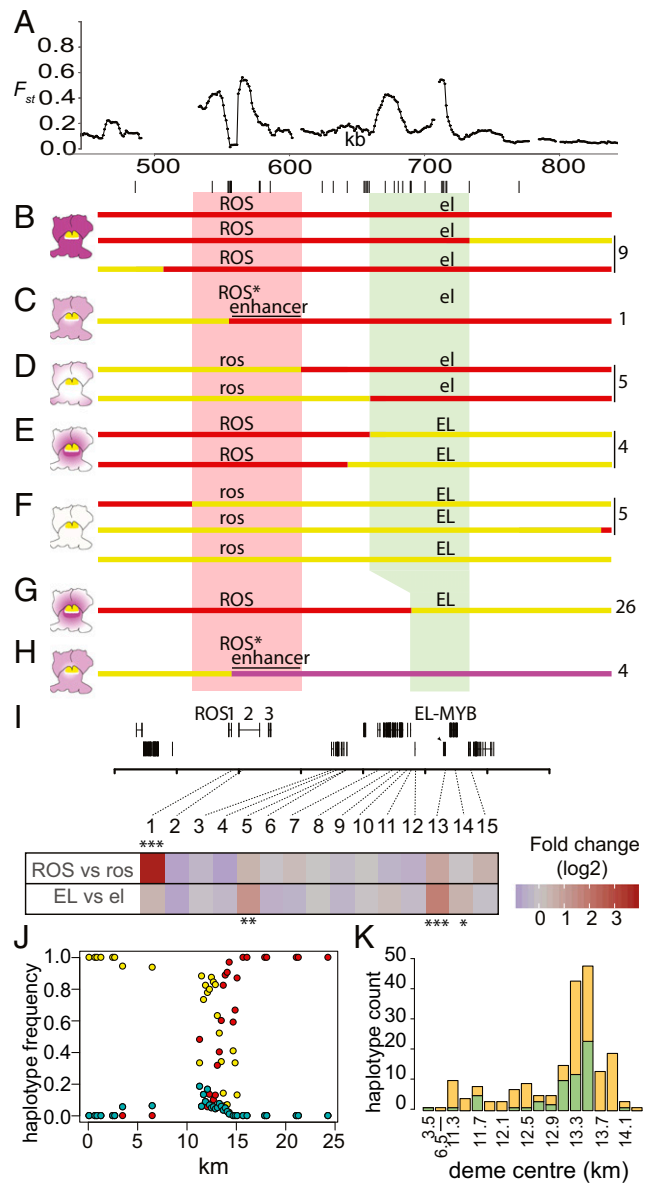


**Fig. 4.** Mapping loci in relation to  $F_{st}$  peaks. (A)  $F_{st}$  profile for pools in Fig. 2 B (YP1 vs. MP2) showing location of genes and markers (lines below) used for mapping. (B–H) Mapping *ROS* and *EL*. Pale red and pale green boxes indicate mapping intervals for *ROS* and *EL*, respectively. Parental haplotypes shown as lines in red (*A. majus* J17), magenta (*A.m.pseudomajus*), or yellow (*A.m.striatum*). Recombination to the left and right of the  $F_{st}$  peak gives parental phenotypes (B and F); recombination 3' of *ROS1* gives pale magenta (C and H); recombination between *ROS* and *EL* gives very pale (D) or restricted (E) patterns. Numbers of each class recovered shown, Right. (I) Floral bud expression of 15 genes found in or between the *ROS* and *EL* mapping intervals. Significant differential expression for *ROS* vs. *ros* or *EL* vs. *el* comparisons at  $q$  (false discovery rate)  $< 0.05$ ,  $q < 0.01$ , and  $q < 0.001$  is indicated by one, two, or three asterisks, respectively. Only genes with a mean expression of  $> 5$  transcripts per million are shown. The sole gene in the region with significant differential expression in *ROS* vs. *ros* comparisons was *ROS1* ( $q < 5.6e^{-29}$ ). *EL-MYB* showed the most significant differential expression in the *EL* vs. *el* comparison ( $q < 2.3e^{-9}$ ) with two further genes (Gene 5, which is outside the mapped *EL* interval) and Gene 14, which is immediately adjacent to *EL-MYB*) reporting differential expression at lower significance thresholds. (J) Frequency of *A.m.pseudomajus* (magenta), *A.m.striatum* (yellow), and recombinant (turquoise) haplotypes in demes with  $\geq 8$  individuals along the hybrid zone transect. (K) Barplot showing counts of recombinant haplotypes for all demes with  $\geq 8$  individuals (*ros<sup>s</sup> e<sup>L</sup>* in green; *ROS<sup>S</sup> EL<sup>S</sup>* in orange). Deme center locations between 11.3 and 14.3 km are at 0.2-km intervals. For details of genotyping, see *SI Appendix*, Supplementary Text S3.





where *A.m.pseudomajus* and *A.m.striatum* populations meet, creating a local barrier to gene flow (28). We performed simulations to explore scenarios consistent with the data and modes of selection.

To provide constraints on simulations, we first estimated the age of the selective sweeps. Based on the residual diversity within the sharp peaks at *ROS* and *EL*, we estimated the date of the most recent sweeps to be  $\sim 90,000$  generations ago (*SI Appendix, Supplementary Text S1*); this is an upper bound, since “soft sweeps” might not have eliminated all diversity. We also estimated the age of the barrier to gene flow. As detailed in *SI Appendix, Supplementary Text S1*, the time required for  $F_{st}$  in the *ROS/EL* interval to accumulate to the observed value of 0.125 is  $T \sim 0.54 N_e \sim 45,000$  generations (where  $N_e$  = effective population size). Thus, both estimates suggest that selective sweeps and a barrier to gene flow were established roughly  $N_e \sim 10^5$  generations ago.

We assume that a homogeneous ancestral population is first split by a geographic barrier, allowing sweeps to occur independently in each population (Fig. 6 *A* and *F*, for simplicity assuming an initial  $F_{st} \sim 0.0$ ). Geographic separation is a simple way of ensuring that alleles swept in one population do not sweep into the other, although other scenarios such as environmental heterogeneity are possible; the sequence data are also compatible with divergence in primary contact. Sweeps at *ROS* and *EL* (red, green in Fig. 6 *B* and *G*) reduce diversity,  $\pi_w$ , generating peaks in  $F_{st}$ . These sweeps presumably reflect the selective advantage of a change in flower color, compared with the ancestral phenotype in each population. Given that both populations underwent sweeps, the ancestral flower phenotype would have been different from both of the current phenotypes in *A.m.pseudomajus* or *A.m.striatum*. Further sweeps at *ROS* and *EL* strengthen the  $F_{st}$  peaks (Fig. 6 *C* and *H*). Unlike the simulations, in real populations, it is possible that global and/or local sweeps occur at many other genetic loci and spatial locations, in addition to *ROS* and *EL*, creating a more rugged  $F_{st}$  profile across the genome.

After a period of time ( $0.2 N_e$  generations in the simulation shown in Fig. 6), the divergent populations come into contact. Gene flow leads to a lowering of  $F_{st}$  from the chromosome-wide average, except at loci where a barrier has been established. We propose that a barrier to gene flow occurs for only a subset of swept loci: those for which epistatic interactions or frequency dependence maintain divergence. *ROS* and *EL* represent one such case, as their interactions, together with loci controlling yellow, lead to alternative floral guides. Other loci that underwent sweeps, but led to no incompatibility (presumably the majority of sweeps) would undergo

gene flow, with the allele conferring higher overall fitness going to fixation in both populations. By time  $0.5 N_e F_{st}$  outside *ROS/EL* has decreased due to gene flow (gray), but has further increased between *ROS* and *EL* (blue) because of the local barrier to gene flow (Fig. 6 *D* and *I*). The resulting  $F_{st}$ ,  $\pi_b$ , and  $\pi_w$  values are comparable to those observed (compare Fig. 6 *D* and *I* with Fig. 6 *E* and *J*). According to the above scenario, selective sweeps led to fixation of different alleles in each population, and selection maintains a local barrier to gene flow. Multiple changes in alleles are involved, a reasonable assumption given these events occurred over a period of  $\sim 10^5$  generations, extending over glacial periods, during which populations and the environment were in a state of flux.

Our analysis indicates that both selective sweeps and barriers to gene flow combine to shape genomic islands of differentiation. The barrier to gene flow at *ROS/EL* is insufficient to prevent exchange for much of the genome. However, if the barrier were more severe and applied to additional loci, it could prevent gene flow more completely, leading to speciation. The mechanisms that created the genomic islands may therefore represent partial steps toward reproductive isolation and speciation.

## Materials and Methods

Full details of plant material, DNA extraction, genome sequence analysis, population genomics, genotyping, SNP analysis for geographic, and RNAseq analysis are given in *SI Appendix, Materials and Methods*. Details on inferences from pairwise diversity and divergence, geographic cline analysis, and genotypic screens are given in *SI Appendix*. Genomic sequence datasets are available at European Nucleotide Archive (ENA) with accession number PRJEB28287, and RNAseq datasets are deposited in National Center for Biotechnology Information (NCBI) Gene Expression Omnibus (GEO) with accession number GSE118621. Associated scripts are provided at linked public data repositories as detailed in *SI Appendix, Materials and Methods*, and further information on the hybrid zone is available at [www.antspec.org](http://www.antspec.org).

**ACKNOWLEDGMENTS.** Many thanks to Christophe Thébaud for sharing his finding of the herbarium specimen referenced in the text. This work was supported by Biotechnology and Biological Sciences Research Council Grants BBS/E/J/000PR9773 and BB/G009325/1 (to E.C.), ERC Grant 201252 (to N.H.B.), and a PhD scholarship (to H.T.) from the Portuguese Foundation for Science and Technology (FCT), through the Human Potential Operating Programme (POPH) of the National Strategic Reference Framework (QREN), within the European Social Fund (Scholarship SFRH/BD/60982/2009). This research was supported in part by the Norwich BioScience Institutes Computing infrastructure for Science (CIS) group.

- Hohenlohe PA, et al. (2010) Population genomics of parallel adaptation in threespine stickleback using sequenced RAD tags. *PLoS Genet* 6:e1000862.
- Martin SH, et al. (2013) Genome-wide evidence for speciation with gene flow in *Heliconius* butterflies. *Genome Res* 23:1817–1828.
- Poelstra JW, et al. (2014) The genomic landscape underlying phenotypic integrity in the face of gene flow in crows. *Science* 344:1410–1414.
- Clarkson CS, et al. (2014) Adaptive introgression between *Anopheles* sibling species eliminates a major genomic island but not reproductive isolation. *Nat Commun* 5:4248.
- Ellegren H, et al. (2012) The genomic landscape of species divergence in *Ficedula* flycatchers. *Nature* 491:756–760.
- Pennisi E (2014) Disputed islands. *Science* 345:611–613.
- Cruikshank TE, Hahn MW (2014) Reanalysis suggests that genomic islands of speciation are due to reduced diversity, not reduced gene flow. *Mol Ecol* 23:3133–3157.
- Ma T, et al. (2018) Ancient polymorphisms and divergence hitchhiking contribute to genomic islands of divergence within a poplar species complex. *Proc Natl Acad Sci USA* 115:E236–E243.
- Wolf JB, Ellegren H (2017) Making sense of genomic islands of differentiation in light of speciation. *Nat Rev Genet* 18:87–100.
- Charlesworth B, Nordborg M, Charlesworth D (1997) The effects of local selection, balanced polymorphism and background selection on equilibrium patterns of genetic diversity in subdivided populations. *Genet Res* 70:155–174.
- Whibley AC, et al. (2006) Evolutionary paths underlying flower color variation in *Antirrhinum*. *Science* 313:963–966.
- Bradley D, et al. (2017) Evolution of flower color pattern through selection on regulatory small RNAs. *Science* 358:925–928.
- Hackbarth J, Michaelis P, Scheller G (1942) Untersuchungen an dem *Antirrhinum*-Wildspalten-Sortiment von E. Baur. *Z Indukt Abstamm Vererbungslehre* 80:1–102.
- Schwinn K, et al. (2006) A small family of MYB-regulatory genes controls floral pigmentation intensity and patterning in the genus *Antirrhinum*. *Plant Cell* 18:831–851.
- Stubbe H (1966) *Genetik und Zytologie von Antirrhinum L. sect. Antirrhinum* (Veb Gustav Fischer Verlag, Jena, Germany).
- Khimoun A, et al. (2012) Ecology predicts parapatric distributions in two closely-related *Antirrhinum majus* subspecies. *Evol Ecol* 27:51–64.
- Shang Y, et al. (2011) The molecular basis for venation patterning of pigmentation and its effect on pollinator attraction in flowers of *Antirrhinum*. *New Phytol* 189:602–615.
- Gegear RJ, Lavery TM (2005) Flower constancy in bumblebees: A test of the trait variability hypothesis. *Anim Behav* 69:939–949.
- Smithson A, Macnair MR (1996) Frequency-dependent selection by pollinators: Mechanisms and consequences with regard to behaviour of bumblebees *Bombus terrestris* (L.) (Hymenoptera: Apidae). *J Evol Biol* 9:571–588.
- Oyama RK, Jones KN, Baum DA (2010) Sympatric sister species of Californian *Antirrhinum* and their transiently specialized pollinators. *Am Midl Nat* 164:337–347.
- Counterterman BA, et al. (2010) Genomic hotspots for adaptation: The population genetics of Müllerian mimicry in *Heliconius erato*. *PLoS Genet* 6:e1000796.
- Mallet J, Barton NH (1989) Strong natural selection in a warning-color hybrid zone. *Evolution* 43:421–431.
- Joron M, Mallet JL (1998) Diversity in mimicry: Paradox or paradigm? *Trends Ecol Evol* 13:461–466.
- Jiggins CD (2017) *The Ecology and Evolution of Heliconius Butterflies* (Oxford Univ Press, Oxford).
- Nadeau NJ, et al. (2012) Genomic islands of divergence in hybridizing *Heliconius* butterflies identified by large-scale targeted sequencing. *Philos Trans R Soc Lond B Biol Sci* 367:343–353.
- Schlötterer C, Tobler R, Kofler R, Nolte V (2014) Sequencing pools of individuals—Mining genome-wide polymorphism data without big funding. *Nat Rev Genet* 15:749–763.
- Payseur BA, Rieseberg LH (2016) A genomic perspective on hybridization and speciation. *Mol Ecol* 25:2337–2360.
- Barton N, Bengtsson BO (1986) The barrier to genetic exchange between hybridising populations. *Heredity (Edinb)* 57:357–376.
- Yeaman S, Aeschbacher S, Bürger R (2016) The evolution of genomic islands by increased establishment probability of linked alleles. *Mol Ecol* 25:2542–2558.